ISSN 1726-5479

SENSORS & TRANSDUCERS

vol. 139
4/12

MEMS and Modern Technologies

International Frequency Sensor Association Publishing

IFSA

Sensors & Transducers

Volume 139, Issue 4, April 2012 | **www.sensorsportal.com** | **ISSN 1726-5479**

Sensors & Transducers Journal (ISSN 1726-5479) is a peer review international journal published monthly online by International Frequency Sensor Association (IFSA).
Available in electronic and on CD.

Sensors & Transducers Journal

Contents

Volume 139
Issue 4
April 2012

www.sensorsportal.com

ISSN 1726-5479

Research Articles

Authors are encouraged to submit article in MS Word (doc) and Acrobat (pdf) formats by e-mail: editor@sensorsportal.com
Please visit journal's webpage with preparation instructions: http://www.sensorsportal.com/HTML/DIGEST/Submition.htm

International Frequency Sensor Association (IFSA).

Sensors & Transducers Journal, Vol. 139, Issue 4, April 2012, pp. 95-108

Sensors & Transducers

ISSN 1726-5479

http://www.sensorsportal.com

Surface Plasmon Resonance Based Fiber Optic Sensor Utilizing Metal Nanoparticles: Influence of Ambient Temperature

[1] Sachin K. SRIVASTAVA, [2] Vikas ARORA, [2] Sameer SAPRA and [*, 1] Banshi D. GUPTA

[1] Department of Physics, Indian Institute of Technology Delhi, New Delhi – 110016, India

[2] Department of Chemistry, Indian Institute of Technology Delhi, New Delhi – 110016, India

[*] Tel.: +91-11-26591355, fax: +91-11-26581114

E-mail: bdgupta@physics.iitd.ernet.in

Received: 9 February 2012 /Accepted: 23 April 2012 /Published: 30 April 2012

Abstract: Influence of ambient temperature on the performance of a localized surface plasmon resonance (LSPR) based fiber optic sensor has been studied, both experimentally and theoretically. The variation of resonance wavelength with change in refractive index confirms the working of the sensor. Water was considered as the sensing medium to study the effect of temperature. A negligible variation in resonance wavelength has been observed for the temperature change in the range 7 – 100 ^{o}C. However, a noticeable change in evanescent absorbance has been observed. The experimental results have been found to be in good agreement with that of theoretical model based on the absorption of evanescent field by the nanoparticles on the core of the fiber. The study implies that the fiber optic LSPR sensor is nearly insensitive to small temperature fluctuations while working in spectral interrogation scheme; however, intensity modulation scheme requires a correction factor for working at different ambient temperatures. *Copyright © 2012 IFSA.*

Keywords: Optical fiber, Surface plasmon, Metal nanoparticle, Sensor, Temperature.

1. Introduction

In recent years, plasmon resonances of various metal nanostructures have got wide attention due to their unique properties in the fields of biochemical sensing, cancer treatment, imaging, waveguiding, and meta-materials [1-4]. Plasmon resonances of metal nanoparticles are called localized surface plasmon resonances (LSPR). The localized surface plasmons (LSPs) are basically the quanta of charge density oscillations, which occur due to the collective oscillations of conduction electrons of metal nanoparticles. These LSPs get resonantly excited when the wavelength of the incident light becomes equal to the characteristic wavelength of the conduction electrons of metal nanoparticle, determined by the LSPR extinction condition [5]. As a result, the metal nanoparticles show a strong absorption at the characteristic wavelength, also termed as resonance wavelength, which is not present in the spectrum of bulk metal. The absorption of light results in the enhancement of local EM field in the vicinity of metal nanoparticle. The absorption band of noble metal nanoparticles generally lies in UV- visible range of electromagnetic spectrum. Thus LSPs in metal nanoparticles can easily be excited by using a tungsten- halogen lamp. The resonance wavelength is a characteristic of the metal of which the nanoparticle is made. It primarily depends on the shape and size of the nanoparticle, in addition to the refractive index of the surrounding medium [6]. If the refractive index of the medium around the metal nanoparticle is increased, the resonance wavelength shows a red shift. This property of metal nanoparticles is utilized in refractive index sensing. A number of studies utilizing the plasmon resonances of metal nanoparticles have been reported in literature [2, 7-9]. The compatibility of attachment of gold nanoparticles with biomolecules, without affecting their properties makes them useful for various biochemical sensing applications [5, 8]. Unlike propagating surface plasmon resonance (pSPR), LSPR does not require a phase matching condition for excitation. Use of metallic nanoparticles in fiber optic sensing probes makes the sensor very cheap and compact. A fiber optic LSPR based refractive index sensor utilizing intensity modulation scheme along with a light emitting diode as a light source has many advantages such as wide sensing range, low cost, and miniaturization [9]. Few studies have reported the fabrication of fiber optic sensing probes utilizing metal nanoparticles for chemical and biochemical sensing [2]. The knowledge of influence of ambient temperature on the performance of a sensor is required to recalibrate the probe according to the temperature of the surrounding medium. The effect of temperature on the sensing of a prism based pSPR sensor using bulk metal film has been reported in literature. In both the cases, angular and spectral interrogation, the sensitivity of a pSPR sensor depends on the ambient temperature [10, 11]. Theoretical reports studying the effect of temperature on pSPR based fiber optic sensors are also available in literature [12]. Neither experimental nor theoretical studies reporting the effect of ambient temperature on the performance of a LSPR based sensor have yet been found in literature. Therefore, the effect of temperature on LSPR based sensing is essential. Also, the need for a universal sensor that can be used in an environment with varying temperature without any change in its sensing parameters and calibration is a well demanded requirement. In view of above points, the present study has been performed to analyze the effect of ambient temperature on the performance of a LSPR based fiber optic refractive index sensor.

In the present article, we report our experimental and theoretical studies on the effect of ambient temperature on the performance of a fiber optic LSPR sensor and discuss the effect of temperature fluctuations on resonance wavelength and evanescent absorbance. Spherical gold nanoparticles were prepared by Turkevich method [13], and a monolayer of these nanoparticles was immobilized on the unclad portion of optical fiber with the help of a self assembled monolayer, which provides strong bonding with the fiber core at one end and with the gold nanoparticle at the other end. Before studying the influence of ambient temperature, the working of the sensor was confirmed by recording LSPR spectra for varying refractive indices around the probe. A red shift in resonance wavelength with increase in the refractive index of the sensing medium confirms the working of the sensor. Further, the absorption spectra were recorded for the sensor at different temperatures of surrounding water. For the theoretical analysis, the temperature dependencies of the dielectric constants of fiber core, metal nanoparticles and sensing medium were considered. The sensor was found to be nearly insensitive to small fluctuations in temperature in spectral interrogation scheme. However, in intensity modulation scheme, the performance of the sensor is noticeably affected by variation in ambient temperature.

2. Experiment

2.1. Materials

Tetrachloroaurate tri-hydrate ($HAuCl_4.3H_2O$) and N-[3-(Trimethoxysilyl)propyl]-ethylenediamine (aminosilane) were purchased from Sigma-Aldrich. Tri-sodium citrate was obtained from Fisher Scientific. Ethanol, glacial acetic acid and sucrose were obtained from Merck. Plastic clad silica (PCS) optical fiber of 600 µm core diameter and 0.4 NA was obtained from Fiberguide Industries.

2.2. Preparation of Nanoparticles

Spherical gold nanoparticles of about 5 nm radius were prepared by using Turkevich method [13]. The 100 ml aqueous solution of tetrachloraurate tri-hydrate ($HAuCl_4.3H_2O$) of 1 mM concentration was boiled with constant stirring. As soon as the boiling commenced, 10 ml of 38.8 mM trisodium citrate solution was added to it. Due to the reduction of $HAuCl_4$, a violet colored solution appeared which slowly turned to brilliant red after half an hour of boiling and stirring. The boiling was stopped and the solution was continuously stirred till it cooled down resulting in the formation of gold nanoparticles uniform size. Citrate ions act as capping agent for gold nanoparticles. A high resolution transmission electron micrograph (HRTEM) of the prepared gold nanoparticles is shown in Fig. 1. The shape of the prepared nanoparticles is spherical and the average size is 10 nm.

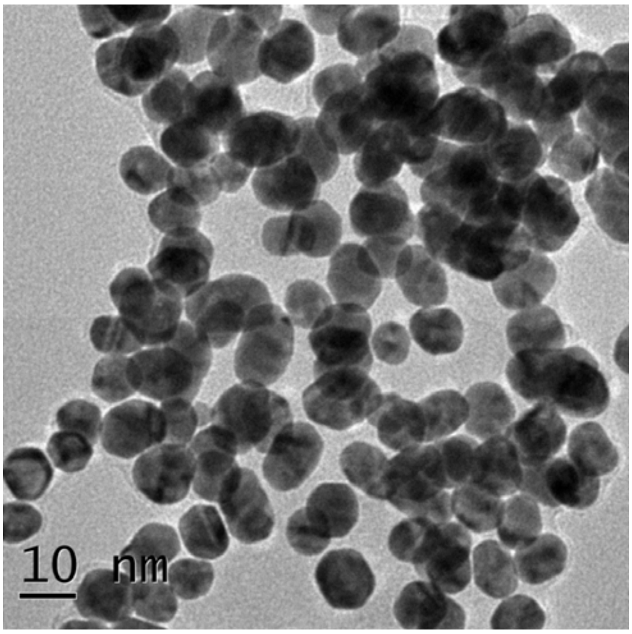

Fig. 1. TEM micrograph of gold nanoparticles.

2.3. Fabrication of Fiber Optic LSPR Probe

To fabricate the sensing probe, 1 cm length of the cladding was removed from the middle of a 20 cm length of the plastic clad silica fiber. The unclad portion of the optical fiber was treated with chromic acid solution (conc. H_2SO_4 + $K_2Cr_2O_7$) for about 30 minutes. The chromic acid excites additional SiOH sites for the binding of aminosilane monomers on the unclad portion of the core of the optical fiber. The optical fiber probe was then washed rigorously with de-ionized water and dried in an oven kept at 110^{o}C for two hours. Gold nanoparticles were attached to the optical fiber by first immobilizing an aminosilane layer and then incubating in the nanoparticle solution. For the formation of a self assembled monolayer of aminosilane a solution of 1 % N-[3-(Trimethoxysilyl)propyl]-ethylenediamine was prepared in a mixture of ethanol and acetic acid (10:4). The unclad portion of optical fiber was then dipped in aminosilane solution for 15 minutes in Ar ambient to form a self assembled monolayer (SAM) on it. Acetic acid stops the formation of aggregates of aminosilane on optical fiber and helps in monomer formation. The optical fiber probe was 4-5 times rinsed with ethanol to remove the unbound monomers from the fiber. This process was repeated thrice for effective binding of aminosilane over the surface of optical fiber. The SAM coated optical fiber was then incubated in citrate capped gold nanoparticle solution for 1 hr for effective binding of gold nanoparticles on it. After the incubation, the fiber was washed with Millipore® water to remove unbound nanoparticles. We repeated this process thrice to ensure the effective binding of the gold nanoparticles and formation of a uniform monolayer.

2.4. Experimental Setup

The working of the sensor was first confirmed before studying the influence of ambient temperature on its performance. An experimental setup similar to that shown in Fig. 2 was used for this study. The fiber optic LSPR probe was fixed in a glass flow cell used for the liquid sample to be kept around the probe. Polychromatic light from a tungsten-halogen (Ava – Hal, Avantes) lamp was launched into the fiber optic LSPR sensor with the help of a microscope objective and a three dimensional translation stage. The light gets guided into the optical fiber due to total internal reflection (TIR) at the core-cladding interface. The evanescent field of the guided light interacts with the nanoparticles to excite localized surface plasmons. Light transmitted off the output end of the fiber was collected by a spectrometer (AvaSpec-3068, Avantes) which records the absorbance spectra. Sucrose solutions of different refractive indices, varying in the range 1.340 to 1.380 were prepared in Millipore® water. The refractive indices of these sample solutions were determined by an Abbe's refractometer, having an accuracy of 0.001 in white light. Sucrose solutions were filled around the sensing region in the flow cell and corresponding LSPR spectra were recorded. The variation of resonance wavelength with refractive index confirms the working of the fabricated sensor. After the working of the sensor was confirmed, the effect of change in ambient temperature was studied.

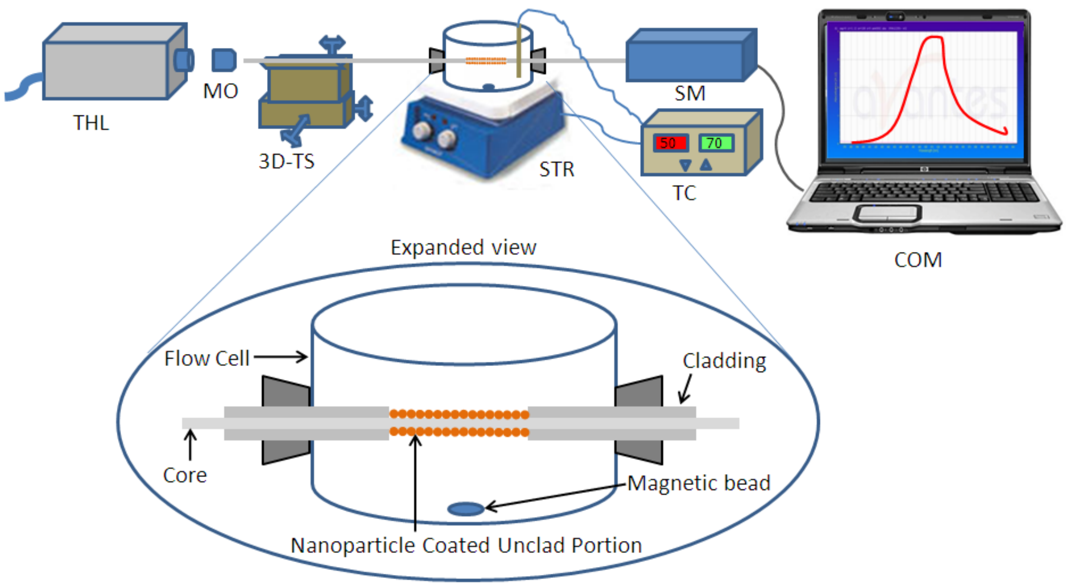

Fig. 2. A schematic of the experimental setup. THL: tungsten-halogen lamp, MO: microscope objective, 3D-TS: 3-dimensional translation stage, STR: stirrer cum heater, TC: temperature controller, SM: spectrometer, COM: personal computer.

For temperature related studies, the flow cell was mounted on a stirrer cum heater and water was filled around the sensing region, as shown in Fig. 2. A thermostat was put in to control the temperature of water around the fiber. The water in the flow cell was slowly stirred to make the temperature uniform throughout the flow cell. Temperature controlled studies of nanoparticle dispersed in water were performed in a temperature controlled sample compartment Qpod® TC 125, purchased from Quantum Northwest.

3. Theory

For theoretical modeling of the fiber optic LSPR sensor we consider the probe shown in Fig. 2. Light launched in the fiber propagates by the phenomenon of total internal reflection (TIR) at the core-cladding interface. The evanescent field of the guided ray in the sensing region interacts with the metal nanoparticles, which results in the wavelength dependent absorption of the evanescent field. The absorption spectrum is determined from the spectral analysis of transmitted power at the output end of the sensing probe. The wavelength corresponding to peak absorption (λ_{res}) in the absorption spectrum depends on the refractive index of the medium surrounding the nanoparticles.

3.1. Effective Evanescent Extinction

If P_o be the power transmitted at the output end of the sensor in the absence of sensing medium, then the power transmitted along the fiber in the presence of sensing medium is given by [14]:

$$P = P_o \exp(-\gamma L), \tag{1}$$

where γ is the evanescent absorption coefficient of the sensing medium and L is the length of the sensing region. The evanescent absorption coefficient of a ray making an angle θ with the normal to the interface is given by [14]:

$$\gamma(\theta,\omega,T) = \frac{NEcn_2 \cos\theta \cot\theta}{\rho L n_1^2 \omega \cos\alpha \cos^2\theta_c (\sin^2\theta - \sin^2\theta_c)^{1/2}}, \tag{2}$$

where E is the extinction of a single metal nanoparticle, ρ is the radius of the core of the fiber, n_2 is the refractive index of the metal nanoparticle, n_1 is the refractive index of the core of the fiber, given by the temperature dependent Sellmeier relation [15], $\theta_c = \sin^{-1}(n_2 / n_1)$ is the critical angle of the sensing region, α is the skewness parameter for the rays that varies from 0 to $\pi/2$ [16], and N is the total number of nanoparticles attached to the bare core of the fiber optic probe. It is given by

$$N = 2\pi\rho L / 4R^2, \tag{3}$$

where R is the radius of the gold nanoparticle. While calculating the total number of nanoparticles, N, we have taken into account the close packing of nanoparticles on the bare core. The area corresponding to a single nanoparticle (πR^2) is replaced by $4R^2$, which is equal to the area of a square of side $2R$. The effective evanescent extinction (or, absorbance) of a single metal nanoparticle is then given by [9]:

$$A(\theta,\omega,T) = \gamma(\theta,\omega,T)L / N \tag{4}$$

3.2. Extinction of a Single Metal Nanoparticle

The extinction cross-section of a nano-sized metal particle is derived by using quasi-static approximation [6]. According the quasi static approximation, the size of the nanoparticle must very much smaller than that of the wavelength of incident light. The temperature (*T*) dependent extinction of a spherical metal nanoparticle of radius *R* is calculated under dipole approximation and is given by [17]:

$$E(\omega,R,T)=\frac{24\pi R\varepsilon_s^{3/2}\varepsilon_2(\omega,R,T)}{\lambda[(\varepsilon_1(\omega,R,T)+2\varepsilon_s)^2+\varepsilon_2^2(\omega,R,T)]} \tag{5}$$

where ε_s is the dielectric constant of the surrounding medium, given by $\varepsilon_s = n^2$, *n* being the refractive index of the surrounding medium, *c* is the speed of light in vacuum, ω is the frequency, ε_1 and ε_2 are the real and imaginary parts of the metal nanoparticle dielectric functions, respectively.

3.3. Temperature Dependence of Metal Nanoparticle Dielectric Function

According to Drude model, the temperature *T* and frequency ω dependent real and imaginary parts of the dielectric functions of a spherical metal nanoparticle of radius *R* are given by [17]:

$$\varepsilon_1(\omega,R,T)=1-\frac{\omega_p^2}{(\omega^2+\omega_c^2)} \tag{6}$$

and

$$\varepsilon_2(\omega,R,T)=\frac{\omega_p^2\omega_c}{\omega(\omega_c^2+\omega^2)} \tag{7}$$

respectively. In above equations, ω_p and ω_c denote the size and temperature dependent plasma and collision frequencies of the nanoparticle, respectively. The temperature dependence of the plasma frequency of the metal nanoparticle is given as [17]:

$$\omega_p(T)=\frac{\omega_{po}}{\sqrt{1+3\alpha(T-T_0)}}, \tag{8}$$

where α (/^{0}K) is the linear thermal expansion coefficient of the metal and ω_{po} is the plasma frequency of metal nanoparticle at reference temperature, T_0, in Kelvin, and is given as [6]:

$$\omega_{po}=\frac{\omega_{pbo}}{\sqrt{3}}, \tag{9}$$

where ω_{pbo} is the bulk plasma frequency at reference temperature. This modification in the plasma frequency of bulk metal due to small size of the nanoparticle is termed as extrinsic size effect. The bulk collision frequency of the metal nanoparticle gets modified with an additional scattering term due to small dimensions. This additional scattering becomes significant when the nanoparticle size becomes comparable to the mean free path of free electrons in the metal. The modification due to the additional scattering is known as intrinsic size effect. Thus, the collision frequency of the metal nanoparticle is given as [6]:

$$\omega_C = \omega_{cb} + \frac{v_f}{R}, \tag{10}$$

where ω_{cb} denotes the bulk collision frequency of the metal and v_f is the speed of conduction electrons at Fermi energy. The collision frequency of bulk metal basically is a sum of two types of scatterings, one corresponding to the phonon - electron collision (ω_{cp}), and the other to the electron - electron collision (ω_{ce}). It is given by

$$\omega_{cb} = \omega_{cp} + \omega_{ce} \tag{11}$$

The contribution of the phonon-electron collision term may be given by the Holstein model as [18]

$$\omega_{cp}(T) = \frac{\dfrac{\omega_p^2 \varepsilon_0}{\sigma(0)}\left[\dfrac{1}{10} + \left(\dfrac{T}{T_D}\right)^5 \displaystyle\int_0^{T_D/T} \dfrac{z^4}{(e^z - 1)} dz\right]}{\left[\displaystyle\int_0^1 \dfrac{z^5}{(e^z - 1)(1 - e^{-z})} dz\right]} \tag{12}$$

where T_D is the Debye temperature, σ(0) is the dc conductivity at $T = T_D$, and ε_o is the permittivity of free space. The derivation of the phonon-electron collision frequency is based on the Debye model for phonon spectrum and is valid under the assumption $k_BT >> E_f$ and $k_BT_D >> E_f$. However, the electron - electron collision frequency is given by Lawrence model as [18]:

$$\omega_{ce}(T) = \frac{1}{6}\pi^4 \frac{\Gamma\Delta}{hE_f}\left[(k_BT)^2 + \left(\frac{h\omega}{4\pi^2}\right)^2\right], \tag{13}$$

where E_f is the Fermi energy of the electrons in the metal, h is the Planck's constant, k_B is the Boltzmann constant, Γ is a constant averaged over the Fermi surface of the scattering probability, and Δ represents the fractional umklapp scattering. The change in the size of metal nanoparticles due to thermal expansion is negligibly small (less than 1%) and hence is not considered in simulations. The values of various parameters considered for the simulation are given in Table 1.

Table 1. Values of various parameters used for simulation.

Parameter	Numerical value
ω_{pbo}	1.3659×10^{16} rad/s
α	1.42×10^{-5} K^{-1}
Γ	0.55
k_B	1.38×10^{-23} J/K
T_D	185 K
Δ	0.77
1/σ(0) at $T = T_D$	1.32×10^{-8} Ωm
E_f	5.53 eV
h	6.625×10^{-34} Js

3.4. Effective Evanescent Absorbance per Nanoparticle

We assume that the light is launched into the fiber from a collimated source using a microscope objective. The power dP arriving at an axial point on the fiber end face between angles θ and $\theta + d\theta$ is given by [16]:

$$dP \propto \frac{n_1^2 \sin\theta\cos\theta}{(1-n_1^2 cos^2\theta)^2} d\theta ,$$

where, θ is the angle of the ray with the normal to the core cladding interface of the fiber. The effective evanescent extinction per nanoparticle (normalized evanescent extinction) for all the guided rays launched into the fiber is then given by [9]:

$$A_{eff} = \frac{\int_{\theta_1}^{\pi/2} A(\theta,\omega,T) \frac{n_1^2 \sin\theta\cos\theta}{(1-n_1^2\cos^2\theta)^2} d\theta}{\int_{\theta_1}^{\pi/2} \frac{n_1^2 \sin\theta\cos\theta}{(1-n_1^2\cos^2\theta)^2} d\theta} \tag{14}$$

where $\theta_1 = \sin^{-1}(n_{cl}/n_1)$; n_{cl} being the refractive index of the fiber cladding. The skewness parameter α is taken equal to zero, as only meridional rays are considered. Such approximations are already found in literature [9, 12].

3.5. Refractive Index of Water

To study the effect of ambient temperature water has been considered as the fluid around the probe. This is because in most of the biochemical and biomedical sensing applications water is preferably used as a solvent. The refractive index of water depends on density, wavelength and temperature. The dependence of the refractive index of water on the above parameters is given in accordance with NIST data set, based on molar refraction in connection with the Lorentz-Lorenz function as [11]:

$$\frac{n^2-1}{n^2+2}\left(\frac{1}{\bar{\rho}}\right) = a_0 + a_1\bar{\rho} + a_2\bar{T} + a_3\bar{\lambda}^2\bar{T} + \frac{a_4}{\bar{\lambda}^2} + \frac{a_5}{\bar{\lambda}^2-\bar{\lambda}_{UV}^2} + \frac{a_6}{\bar{\lambda}^2-\bar{\lambda}_{IR}^2} + a_7\bar{\lambda}^2 \tag{15}$$

where a_0 to a_7, $\bar{\lambda}_{UV}$ and $\bar{\lambda}_{IR}$ are constants with values 0.244257733, 9.74634476×10^{-3}, -3.73234996×10^{-3}, -3.73234996×10^{-3}, 1.58920570×10^{-3}, 2.45934259×10^{-3}, 0.900704920, -1.66626219×10^{-2}, 0.229202 and 5.432937, respectively and the terms $\bar{\rho}$, $\bar{T}$ and $\bar{\lambda}$ are dimensionless variables given by $\bar{\rho} = \rho/\rho^*$, $\bar{T} = T/T^*$ and $\bar{\lambda} = \lambda/\lambda^*$; where, $\rho^* = 1000$ Kg/m^3, $T^* = 273.15$ K and $\lambda^* = 0.589$ μm, and ρ, T and λ denote the density, temperature and wavelength, respectively.

4. Results and Discussion

Before studying the effect of ambient temperature on the resonance wavelength, we have studied the performance of the fabricated LSPR probe for different refractive indices. The absorbance spectra were recorded for aqueous sucrose solutions of different refractive indices around the probe. The results obtained are shown in Fig. 3.

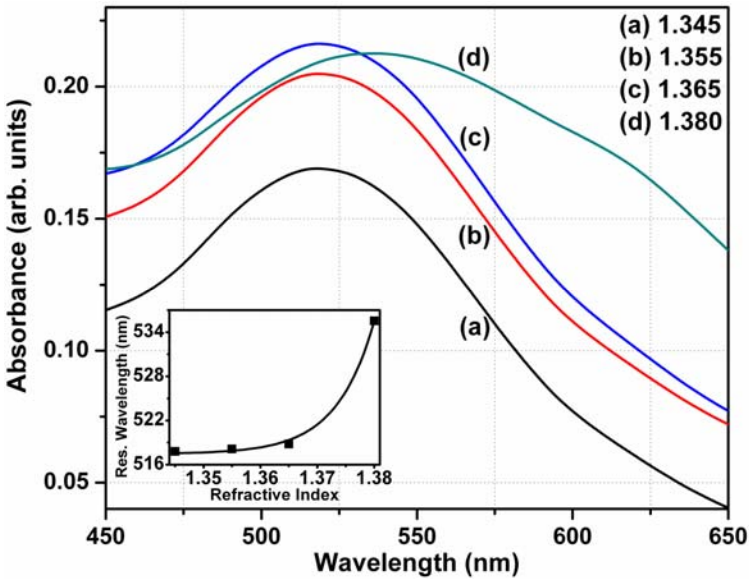

Fig. 3. LSPR spectra of fiber optic sensor for different refractive indices of the medium around the probe. The inset shows the variation of resonance wavelength with refractive index.

It is observed from the spectrum that for each sample solution, the absorption becomes a maximum at some particular wavelength. The wavelength corresponding to the maximum absorbance is termed as resonance wavelength and is a characteristic of the sample solution filled around the sensing region. As the refractive index of the sample solution was increased, a red shift in the resonance wavelength was observed. This can be seen more clearly in the inset. These observations confirmed the working of the sensor and the immobilization of nanoparticles over the core of the fiber.

To see the effect of ambient temperature, following two kinds of experiments have been performed: (1) gold nanoparticles uniformly dispersed in water, and (2) gold nanoparticles immobilized on the fiber core with water as a surrounding medium around it. In the first case we measure the bulk absorbance as a function of wavelength, while in the second case it is the evanescent absorbance of metal nanoparticles immobilized on the optical fiber. The experimental results showing the variation of absorbance/evanescent absorbance with wavelength (λ) at different temperatures varying from 7 ^{o}C to 100 ^{o}C in these two cases have been shown in Figs. 4 (a) and (b) respectively. It is observed from the figures that the resonance maxima for the fabricated sensor are slightly red shifted than that of nanoparticles in bulk water. This is in accordance with previous studies, which report a red shift in the LSPR wavelength due to mutual interactions of immobilized nanoparticles [19]. It is also observed from Figs. 4 (a) and (b) that the extinction of the nanoparticle decreases slightly with increase in temperature, while the position of the resonance wavelength remains unchanged. This implies that the performance of a fiber optic LSPR sensor in spectral interrogation scheme is unaffected by fluctuations in the ambient temperature. The experimental observations were further supported by simulations. We have calculated the effective evanescent absorbance per nanoparticle (A_{eff}) for the sensor as a function of wavelength for water as a sensing medium, kept at different temperatures. Inter-particle interactions have not been considered in the simulations to present a simple analysis and therefore evanescent absorbance per nanoparticle has been determined. Also, the aminosilane SAM has also been ignored because its thickness is very small, only a few angstroms. The simulations therefore present only a qualitative analysis of the present sensor. The numerical aperture and the core diameter of the optical fiber were considered as 0.4 and 600 μm, respectively for simulations.

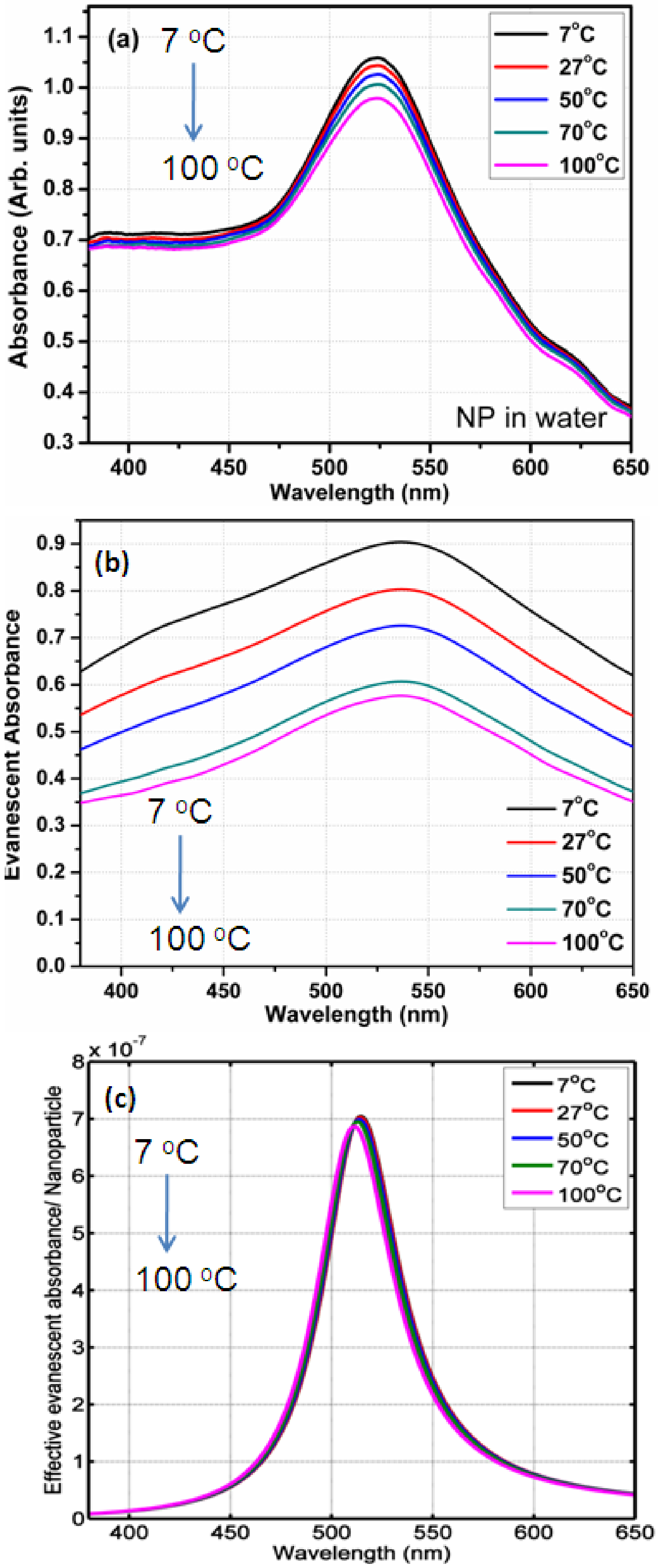

Fig. 4. LSPR spectra at different temperatures for water as a sensing medium: (a) Experimental curves for nanoparticles dispersed in water; (b) experimental curves for nanoparticles immobilized on the fiber core, and (c) simulated curves for nanoparticles immobilized on fiber core.

Fig. 4 (c) shows the simulated evanescent absorbance spectra for a single nanoparticle of the fiber optic LSPR probe with water as a sensing medium at different temperatures. The spectra shown in Figs. 4 (a) to (c) are slightly different in shape. This may be due to different environmental conditions in two experiments and approximations taken in simulation, such as non inclusion of skew rays etc. In fact, the LSPR spectra of nanoparticle immobilized by a SAM layer have been found to be broader than that for nanoparticles uniformly dispersed in some medium [2]. Also, we have plotted only the evanescent absorbance spectra for a single nanoparticle in Fig. 4(c), where the interactions between nanoparticles have not been considered and calculations have been carried out only for meridional rays.

To see the variation of resonance wavelength with temperature more precisely, the resonance wavelengths, characterized by the maximum absorbance/evanescent extinction were determined from these spectra at different temperatures. We have plotted the variation of resonance wavelength with temperature in Fig. 5 for all the three cases. Filled circles correspond to the case when the nanoparticles are uniformly dispersed in bulk water, filled triangles correspond to the experiments carried out when nanoparticles are immobilized on the fiber core and filled squares correspond to the simulated results related to fiber optic LSPR sensor. As can be seen from this figure, the blue shift in resonance wavelength with temperature is almost negligible in the case when the nanoparticles are dispersed in water. Similarly, in the case of fiber optic LSPR sensor there is a negligibly small blue shift in resonance wavelength with temperature in both the experimental and theoretical studies. Though the simulations have been carried out only for the evanescent absorbance of a single nanoparticle, simulated results show good qualitative agreement with the experimental ones. The difference between the resonance wavelengths of experimental and simulated spectra may be due to the approximations considered in the theoretical model. However, the variation in resonance wavelength is very small. For a change of temperature from 7 to 100 ^{o}C it is less than 3 nm. The insignificant effect of ambient temperature on the performance of a localized surface plasmon resonance based fiber optic refractive index sensor in spectral interrogation scheme implies that it does not need recalibration if there is a temperature change of environment or even if there is a fluctuation in the temperature.

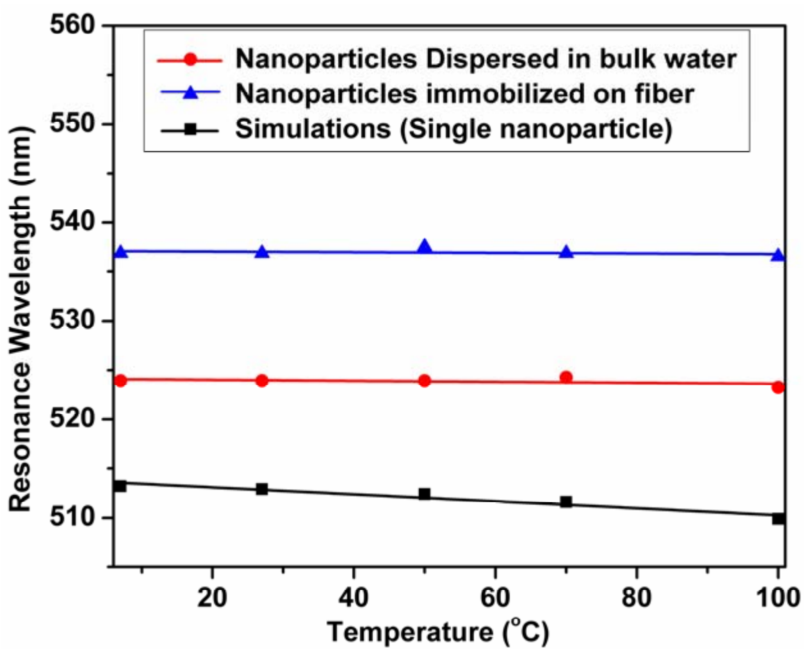

Fig. 5. Experimental and simulated results for the variation of resonance wavelength with the temperature of the water as the sensing medium.

To quantify the influence of ambient temperature on the performance of the sensor in intensity modulation scheme, we have plotted the change in absorbance at various temperatures with reference to 7 °C ($A_t - A_7$) with increase in temperature in Fig. 6 for the above discussed three cases. It is observed that the change in absorbance (At-A7) is greater for the nanoparticles immobilized on optical fiber than that in bulk water. Such a variation may be due to the temperature and wavelength dependence of the refractive index of the optical fiber core. Also, a red shit in LSPR spectra is observed for the nanoparticles immobilized on the optical fiber than that in bulk water. Since the penetration depth of the evanescent field increases with an increase in the wavelength, the absorbance of the evanescent power is more in the case of immobilized nanoparticles. Simulations again show a good qualitative match of the change in absorbance ($A_t - A_7$) with temperature for a single nanoparticle as the change in absorbance ($A_t - A_7$) increases with increase in temperature in this case also. If ($A_t - A_7$) is to be accounted for all the nanoparticles immobilized on the optical fiber, then the terms representing mutual interactions between the nanoparticles and skew rays must be incorporated into simulations. The simulated response curve then may approach towards that of the fabricated LSPR probe. However, it can be clearly predicted from both the experimental and simulated LSPR spectra that the performance of the fiber optic LSPR sensor is greatly affected by the change in ambient temperature. This is an important issue, as sensors fabricated and calibrated in western countries will not be useful in eastern ones due to the differences in ambient temperature and vice versa. Therefore, the present sensor is useful in spectral interrogation scheme, as its performance is not affected by the ambient temperature. However, for its use in intensity modulation scheme, another temperature monitoring system with temperature compensation electronics is also required which performs online temperature measurements and nullifies the effect of ambient temperature on its refractive index sensing. This may be understood by analogy of fiber Bragg gratings used for strain measurements, which require another sensor which simultaneously measures temperature and compensates the temperature effects on strain sensing and vice versa. The present study is significant for the advent and development of a sensor whose performance is not affected by small fluctuations in ambient temperature.

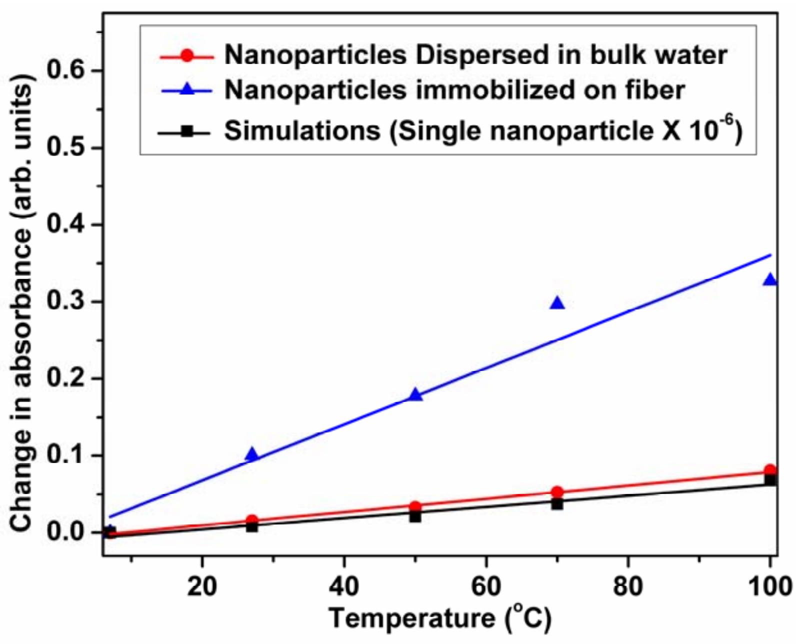

Fig. 6. Variation of difference in absorbance ($A_t - A_7$) at any temperature with reference to 7 °C with temperature.

5. Conclusions

In the present study, we have, experimentally, studied the effect of ambient temperature on the performance of a localized surface plasmon resonance based fiber optic refractive index sensor. The influence of ambient temperature has been found to be negligible in the spectral interrogation scheme of operation. However, in intensity modulation scheme, the performance of the sensor is reasonably affected. These results were further supported by simulations carried out using evanescent field absorption model and the experiments carried out on nanoparticles dispersed in water. The present study provides a platform for use of such sensors in various modes of operation. In intensity modulation scheme, the sensor must be accompanied by a temperature calibrating electronics, which takes account of effect of temperature on the sensor while measuring refractive indices with it.

Acknowledgements

The present research is partially supported by the Department of Science and Technology India. S. K. Srivastava and V. Arora thank Council of Scientific and Industrial Research India for fellowship.

References

[1]. R. Bardhan, S. Lal, A. Joshi and N. J. Halas, Theranostic nanoshells: From probe design to imaging and treatment of cancer, *Accounts of Chemical Research*, Vol. 44, 2011, pp. 936-946.

[2]. L.-K. Chau, Y.-F. Lin, S.-F. Cheng and T.-J. Lin, Fiber-optic chemical and biochemical probes based on localized surface plasmon resonance, *Sensors and Actuators B*, Vol. 113, 2006, pp. 100-105.

[3]. A. V. Kabashin, P. Evans, S. Pastkovsky, W. Hendren, G. A. Wurtz, R. Atkinson, R. Pollard, V. A. Podolskiy and A. V. Zayats, Plasmonic nanorod metamaterials for biosensing, *Nature Materials*, Vol. 8, 2009, pp. 867-871.

[4]. B. Lee, I.–M. Lee, S. Kim, D.–H. Oh, and L. Hesselink, Review on subwavelength confinement of light with plasmonics, *Journal of Modern Optics*, Vol. 57, 2010, pp. 1479-1497.

[5]. E. Hutter and J. H. Fndler, Exploitation of localized surface plasmon resonance, *Advanced Materials*, Vol. 16, 2004, pp. 1685-1706.

[6]. P. Mulvaney, Surface plasmon spectroscopy of nanosized metal particles, *Langmuir*, Vol. 12, 1996, pp. 788-800.

[7]. A. J. Haes and R. P. V. Duyne, A unified view of propagating and localized surface plasmon resonance biosensors, *Analytical and Bioanalytical Chemistry*, Vol. 379, 2004, pp. 920-930.

[8]. A. K. Sharma and B. D. Gupta, Fibre-optic sensor based on surface plasmon resonance with Ag-Au alloy nanoparticle films, *Nanotechnology*, Vol. 17, 2006, pp. 124.

[9]. S. K. Srivastava, R. K. Verma and B. D. Gupta, Theoretical modeling of a localized surface plasmon resonance based intensity modulated fiber optic refractive index sensor, *Applied Optics*, Vol. 48, 2009, pp. 3796-3802.

[10]. Ş. K. Özdemir, and G. T. Sayan, Temperature effects on surface plasmon resonance: Design considerations for an optical temperature sensor, *Journal of Lightwave Technology*, Vol. 21, 2003, pp. 805-814.

[11]. C. S. Moreira, A. M. N. Lima, H. Neff and C. Thirstrup, Temperature dependent sensitivity of surface plasmon resonance sensors at the gold-water interface, *Sensors and Actuators B*, Vol. 134, 2008, pp. 854-862.

[12]. A. K. Sharma, and B. D. Gupta, Influence of temperature on the sensitivity and signal-to-noise ratio of a fiber-optic surface-plasmon resonance sensor, *Applied Optics*, Vol. 45, 2006, pp. 151-161.

[13]. J. Turkevich, P. C. Stevenson and J. Hillier, A study of the nucleation and growth processes in the synthesis of colloidal gold, *Discussions of the Faraday Society*, Vol. 11, 1951, pp. 55-75.

[14]. B. D. Gupta, A. Sharma and C. D. Singh, Evanescent wave absorption wave sensors based on uniform and tapered fibers, *International Journal of Optoelectronics*, Vol. 8, 1983, pp. 409-418.

[15]. G. Ghosh and M. Endo, Temperature-dependent Sellmeier coefficients and chromatic dispersions for some optical fiber glasses, *Journal of Lightwave Technology*, Vol. 12, 1994, pp. 1338-1341.

[16]. A. W. Snyder and J. D. Love, Optical Waveguide Theory, *Chapman & Hall*, 1985.
[17]. S. K. Srivastava, and B. D. Gupta, Simulation of a localized surface plasmon resonance based fiber optic temperature sensor, *Journal of Optical Society of America A*, Vol. 27, 2010, pp. 1743-1749.
[18]. L. Gao and Z.-Y. Li, Temperature dependence of nonlinear optical properties in metal/dielectric composites, *Physica Status Solidi (B)*, Vol. 218, 2000, pp. 571-582.
[19]. S. A. Maier, Plasmonics: Fundamentals and Applications, *Springer*, 2007.

Guide for Contributors

Aims and Scope

Sensors & Transducers Journal (ISSN 1726-5479) provides an advanced forum for the science and technology of physical, chemical sensors and biosensors. It publishes state-of-the-art reviews, regular research and application specific papers, short notes, letters to Editor and sensors related books reviews as well as academic, practical and commercial information of interest to its readership. Because of it is a peer reviewed international journal, papers rapidly published in *Sensors & Transducers Journal* will receive a very high publicity. The journal is published monthly as twelve issues per year by International Frequency Sensor Association (IFSA). In additional, some special sponsored and conference issues published annually. *Sensors & Transducers Journal* is indexed and abstracted very quickly by Chemical Abstracts, IndexCopernicus Journals Master List, Open J-Gate, Google Scholar, etc. Since 2011 the journal is covered and indexed (including a Scopus, Embase, Engineering Village and Reaxys) in Elsevier products.

Topics Covered

Contributions are invited on all aspects of research, development and application of the science and technology of sensors, transducers and sensor instrumentations. Topics include, but are not restricted to:

- Physical, chemical and biosensors;
- Digital, frequency, period, duty-cycle, time interval, PWM, pulse number output sensors and transducers;
- Theory, principles, effects, design, standardization and modeling;
- Smart sensors and systems;
- Sensor instrumentation;
- Virtual instruments;
- Sensors interfaces, buses and networks;
- Signal processing;
- Frequency (period, duty-cycle)-to-digital converters, ADC;
- Technologies and materials;
- Nanosensors;
- Microsystems;
- Applications.

Submission of papers

Articles should be written in English. Authors are invited to submit by e-mail editor@sensorsportal.com 8-14 pages article (including abstract, illustrations (color or grayscale), photos and references) in both: MS Word (doc) and Acrobat (pdf) formats. Detailed preparation instructions, paper example and template of manuscript are available from the journal's webpage: http://www.sensorsportal.com/HTML/DIGEST/Submition.htm Authors must follow the instructions strictly when submitting their manuscripts.

Advertising Information